

Article

Activation Mechanism of Lead Ions in Perovskite Flotation with Octyl Hydroxamic Acid Collector

Yu Zheng ¹, Yating Cui ¹ and Weiqing Wang ^{1,2,*}

¹ School of Environment and Resource, Southwest University of Science and Technology, Mianyang 621010, Sichuan, China; swustzy@126.com (Y.Z.); swustcyt@163.com (Y.C.)

² Key Laboratory of Solid Waste Treatment and Resource Recycle, Ministry of Education, Southwest University of Science and Technology, Mianyang 621010, Sichuan, China

* Correspondence: wangweiqing@swust.edu.cn; Tel.: +86-816-241-9569

Received: 5 July 2018; Accepted: 4 August 2018; Published: 8 August 2018



Abstract: The activation mechanism of lead ions (Pb^{2+}) in perovskite flotation with an octyl hydroxamic acid collector was systematically investigated using microflotation experiments, zeta-potential measurements, adsorption tests, Fourier transform infrared (FT-IR) analysis, and X-ray photoelectron spectroscopy (XPS) analysis. The results of microflotation experiments and adsorption tests indicate that the presence of Pb^{2+} can promote the adsorption of octyl hydroxamic acid (OHA) on the perovskite surface and enhance the flotability of perovskite under weakly acidic conditions. The maximum recovery of 79.62% was obtained at pH 6.5 in the presence of Pb^{2+} , and the maximum recovery of 57.93% was obtained at pH 5.7 without Pb^{2+} . At pHs below 7, lead species are mainly present as Pb^{2+} and $PbOH^+$ in the solution; besides this, the relative content of titanium increases on the perovskite surface. The adsorption of Pb^{2+} and $PbOH^+$ on the perovskite surface makes the zeta-potential of perovskite shift positively, and increases the number of activated sites on the perovskite surface. FT-IR and XPS analyses confirm that OHA chemisorbs on the surface of Pb^{2+} -activated perovskite and forms hydrophobic Pb-OHA complexes, which improve the flotability of perovskite.

Keywords: perovskite; flotation; octyl hydroxamic acid; lead ions; activation

1. Introduction

Titanium and titanium alloys have extensive applications, such as in aerospace, national defense, transportation, medical devices, and national economic production as important strategic resources [1–5]. Ilmenite ($TiFeO_3$) is used as the raw material for titanium production because of the relative scarcity of rutile (TiO_2) [6,7].

More than 95% of China's titanium resource deposits are distributed over the PanXi area (Panzhihua and Xichang, Sichuan province), which mostly exists in vanadium–titanium magnetite ore [4,5,8,9]. When vanadium–titanium magnetite concentrate is smelted in a blast furnace, the titanium is mostly concentrated in the perovskite phase (mainly $CaTiO_3$) of blast furnace slag in the process of PanXi iron-smelting. The blast furnace slag is an important synthetic titanium resource, with a TiO_2 grade of approximately 20–25% [10–12]. At present, the annual production of titanium-bearing blast furnace slag is more than 3.0×10^6 tons; a large amount of slag accumulation leads to the waste of titanium resources and serious environmental pollution [13].

Perovskite can be used as a starting ore for titanium production. Some studies have investigated the reduction of Ti metals starting from $CaTiO_3$ instead of TiO_2 , and obtained success [7,14]. In industry, various methods are used to recycle qualified perovskite product, such as gravity separation, magnetic separation, smelting reduction, and hydrometallurgy [11,15,16]. However, because perovskite is

disseminated in gangue minerals in fine grains (<10 μm), flotation separation is the most common method for the effective separation of perovskites from gangue minerals [17]. Previous studies on perovskite have indicated that, compared with ilmenite and rutile, perovskite exhibits poor flotability under typical flotation conditions [1,17].

It has been reported that sodium oleate and sodium lauryl sulfate were used as collectors for perovskite flotation; nonetheless, because of their poor selectivity, it is difficult to separate and recover perovskite effectively [18]. Alkyl hydroxamic acid collectors are widely used for the flotation of iron, tin, and rare earth metal minerals because of their high selectivity [19–25]. For instance, octyl hydroxamic acid (OHA) can be adsorbed on the surface of monazite selectively and recover rare earth oxides from hematite, quartz and calcite [26–29]. In addition, because the reactivity between lead ions and hydroxamic acid collectors is more extreme than other metal ions, lead ions are often used with hydroxamic acid collectors [30]. For example, lead ions can be adsorbed onto an ilmenite surface and complexed with benzohydroxamic acid in solution, which significantly improves the recovery of ilmenite [30]. Previous studies have demonstrated the effectiveness of lead ion activation [31–35]. However, when octyl hydroxamic acid is used as the collector, the effect of lead ions on perovskite flotation has not yet been reported. Herein, Pb^{2+} is introduced as an activator of perovskite flotation to overcome the poor flotability of perovskites.

The objective of this study is to explore the effects of lead ions on perovskite flotability and the activation mechanism of lead ions in perovskite flotation with octyl hydroxamic acid collector through microflotation experiments, zeta-potential measurements, adsorption tests, FT-IR analysis and XPS analysis.

2. Materials and Methods

2.1. Materials and Reagents

Because perovskite has a fine grain size (<10 μm) and a complex association with gangue minerals in blast furnace slag, it is difficult to separate pure minerals by physical methods [17]. Thus, equivalent amounts of CaO and TiO_2 were mixed and heated at 1350 $^\circ\text{C}$ for 10 h to obtain perovskite [36]. After being ground and screened, 38–75 μm of powdered samples were used in the flotation experiments [17]. The samples used for the zeta-potential measurements and FT-IR analysis were further ground to about 2 μm . The chemical composition and X-ray diffraction (XRD) results of the perovskite sample used in the present study are shown in Table 1 and Figure 1, respectively. The results indicate that the prepared perovskite is very pure.

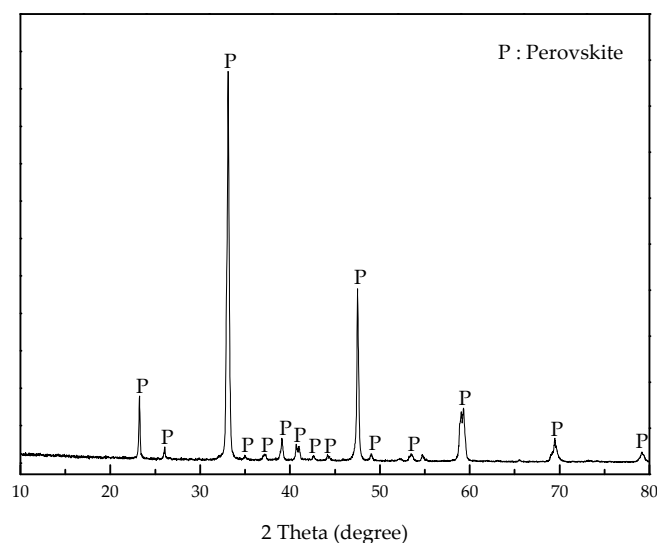


Figure 1. XRD spectrum of perovskite sample.

Table 1. Chemical composition of perovskite sample (mass fraction, %).

Sample	TiO ₂	CaO	Total
Perovskite	58.77	41.23	100.00

In this study, the OHA collector and activator Pb(NO₃)₂ were chemically pure. Perovskite was washed to neutrality with deionized water and then dried at 60 °C before flotation. Hydrochloric acid (HCl) and sodium hydroxide (NaOH) were used to adjust the pH of the system. Deionized water (resistivity: 18.25 MΩ·cm) was used for the microflotation experiments and subsequent measurements.

2.2. Microflotation Experiments

Microflotation experiments were conducted in a 40 mL hitch groove flotation cell. At first, 2.0 g of the mineral sample and 35 mL of deionized water were placed in the plexiglass cell and then agitated for 1 min. Next, the pH of the pulp was adjusted by HCl or NaOH and agitated for 3 min. Then, the Pb(NO₃)₂ was added and agitated for an additional 3 min. After that, the OHA was added and agitated for 3 min, and the pH of the suspension was recorded before the collection. Finally, the froth products were collected for 4 min. The recoveries were calculated based on the dry weight of products. Three measurements in the microflotation experiments were performed, and the averages were recorded.

2.3. Zeta-Potential Measurements

The zeta-potentials were measured using a Zetasizer Nano Zs90 (Malvern Instruments, Malvern, UK) at room temperature (25 °C). The zeta-potentials were monitored continuously based on the conductivity and pH of the suspension during the measurements. Thirty milligrams of the perovskite sample was put into 50 mL of electrolyte solution (1 mM KCl) to prepare the suspensions. The prepared suspension was conditioned by magnetic stirring for 5 min, during which the pH of the suspension was measured. After settling for 10 min, the supernatant of the dilute fine particle suspension was obtained for zeta-potential measurements. The final results were averaged over three measurements.

2.4. FT-IR Spectroscopy Analysis

The FT-IR spectra were obtained from 4000 to 400 cm⁻¹ using a Spectrum One (version BM) spectrometer (Perkin Elmer, Waltham, MA, USA) at 25 °C. Two grams of the perovskite sample was ground to a diameter of less than 2 μm, and then combined with suitable reagents in a plexiglass cell and conditioned for 40 min. Subsequently, the solid sample was washed three times using deionized water at the same pH. The washed samples for FT-IR analysis were vacuum-dried at 60 °C. Approximately 5% (mass fraction) of the solid sample was mixed with spectroscopic grade KBr to obtain the spectra of the solids.

2.5. Adsorption Tests

The amount of OHA adsorbed on the surface of perovskite was determined at 25 °C by spectrophotometer (UV-2600, Shimadzu, Kyoto, Japan). First, 2.0 g of mineral sample and 35 mL of deionized water were placed in the plexiglass cell, and then the reagents were added into the suspension. Next, the suspension was fixed to 50 mL with deionized water. The suspension was shaken at 25 °C for 12 h. The supernatant of the dilute fine particle suspension was obtained for adsorption tests. The adsorbed amount of OHA on the perovskite surface was calculated using the following Equation (1):

$$\Gamma = (C_0 - C) \times V / (mA), \quad (1)$$

where Γ is the adsorbed amount of OHA on the perovskite surface (mol/m²); C_0 and C are the concentrations of OHA in initial and supernatant, respectively (mol/L); V is the volume of the solution

(L); m is the weight of perovskite particles (g); and A is the mineral specific surface area (m^2/g). The final results were averaged over three measurements.

2.6. XPS Analysis

A Kratos AXIS Ultra XPS system equipped with a monochromatic Al X-ray source, operated at 150 W (the energy resolution is 0.48 eV (Ag 3d_{5/2}) and the error value is 0.05 eV), was used to perform XPS measurements. Survey scans were conducted in a single sweep from 0 to 1350 eV, with a dwell time of 8 s, a passing energy of 150 eV, and a 1-eV step size. For high-resolution scanning, the number of scans was increased, the dwell time was reduced to 0.5 s, and the band pass energy was adjusted to 30 eV. The purified mineral particles (2.0 g) and deionized water (35 mL) were placed in the plexiglass cell, and then adjusted with appropriate reagents. Subsequently, the solid samples were washed three times with deionized water. The washed samples for XPS analysis were vacuum-dried at 60 °C.

3. Results

3.1. Microflotation Experiments

Figure 2 shows the flotation recovery of the perovskite as functions of pH using OHA as the collector in the presence and absence of Pb^{2+} . The recovery of perovskite first increased and then decreased with increasing pH in the presence and absence of Pb^{2+} . When only OHA was used, the flotation recovery reached a maximum of about 57.93% at approximately pH 5.70. However, after adding Pb^{2+} into the slurry, the flotation recovery was significantly increased throughout the investigated pH range, and the maximum recovery of 79.62% occurred at approximately pH 6.5. The results indicate that the presence of Pb^{2+} has a positive effect on the perovskite flotation using OHA.

Figure 3 displays the effect of Pb^{2+} concentration on perovskite flotation recovery. With the increase of Pb^{2+} concentration, the flotation recovery of perovskite increased gradually and achieved 79.62% at Pb^{2+} concentration of 0.1 mM. After that, the flotation recovery of perovskite showed no obvious change when Pb^{2+} concentration was more than 0.1 mM. Thus, the optimum conditions (Pb^{2+} concentration: 0.1 mM, pH: 6.54) for perovskite flotation determined by flotation results could be used for subsequent experiments.

Previous studies have shown that in a weakly acidic environment, calcium ions on the perovskite surface are largely dissolved into the slurry, and titanium on the perovskite surface becomes the main site for hydroxamic acid [17]. Compared with calcium ions, titanium ions and hydroxamic acid have a stronger effect [37–39]. These factors explain why the highest flotation recovery is under weak acidic conditions when OHA is used as a collector for perovskite.

According to the ionization constant $\text{p}K_{\alpha}$ of OHA $\cong 9$ [17,40], the concentration logarithmic of each component in different pH solutions of OHA can be calculated. The logarithmic diagram of OHA hydrolysis components as functions of pH when the OHA concentration is 0.2 mM are presented in Figure 4. It can be seen that the molecular OHA concentration decreases and the concentration of ionic OHA increases as the pH of the pulp increases. When the pH is less than 9, the OHA molecule is the main component in the flotation slurry, and the OHA anion is the minor component. In OHA solution, OHA anions and OHA molecules can be adsorbed on the mineral surface, they can chelate with the metal cations on the mineral surface, and the nonpolar part of OHA species can be adsorbed on the nonpolar part of the former OHA species through hydrogen bonds [17,19].

Therefore, at a pH of about 6.5, the multi-layer adsorption of OHA species and the relative increase of the perovskite surface's active metal cations significantly increase the flotability of the perovskite [39–43].

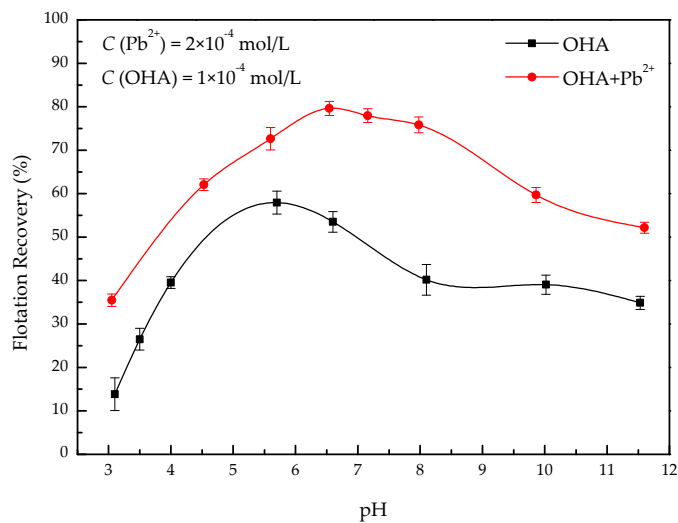


Figure 2. Effects of pH on perovskite flotation recovery in the absence and presence of Pb²⁺.

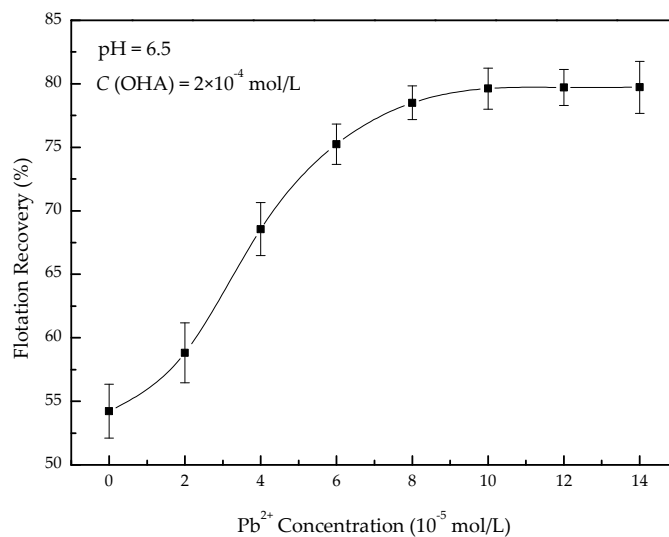


Figure 3. Effects of Pb²⁺ concentration on perovskite flotation recovery.

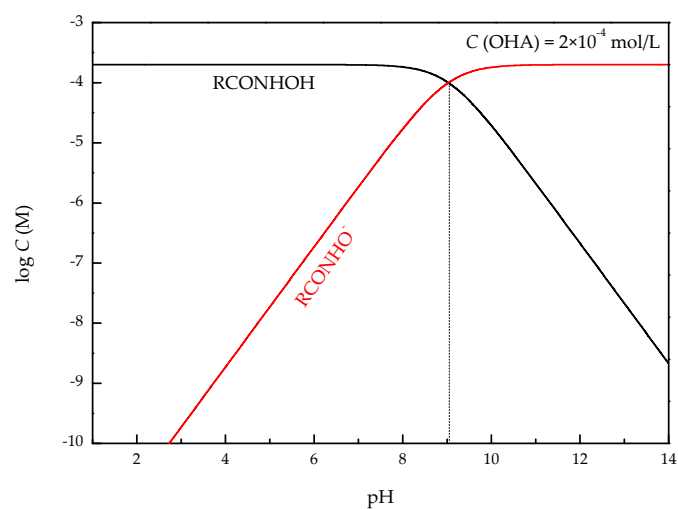


Figure 4. Logarithmic diagram of octyl hydroxamic acid (OHA) hydrolysis components.

3.2. Zeta-Potential Measurements

Figure 5 presents the effect of Pb^{2+} and OHA on the zeta-potential of perovskite. The isoelectric point (IEP) of perovskite was found to be pH 4.1, which is in accordance with previous reports [17]. After the OHA was added to the slurry, the zeta-potential of the perovskite was reduced, and the isoelectric point was moved to 2.9. Therefore, it could be concluded that a specific adsorption of OHA species on the perovskite surface occurred. The research has shown that the adsorption of OHA on the perovskite surface may occur through chemical adsorption [17,30]. When Pb^{2+} was added to the suspension, the zeta-potential increased significantly at the investigated pH, and the maximum zeta-potential was observed at pH 7.3.

According to the solubility product pK_{sp} of $Pb^{2+} \cong 15.2$ [30,43], the solution chemistry of OHA can be calculated to generate the concentration logarithmic diagram of each component in different pH solutions. Figure 6 shows the $\log C$ -pH of the Pb^{2+} hydrolysis components as functions of pH when the Pb^{2+} concentration is 0.1 mM. It can be observed from Figure 6 that lead is mainly present as Pb^{2+} at low pHs. As the pH increased, the concentration of $PbOH^+$ increased gradually. Previous studies have shown that Pb^{2+} and $PbOH^+$ have a high activity and are adsorbed on the surface of minerals by chemical adsorption [21,30]. When the pH was 6–9, the concentrations of $PbOH^+$ and Pb^{2+} are both high; this might explain why the maximum zeta-potential is at pH 7.3. In the presence of Pb^{2+} and OHA, the perovskite zeta-potential is lower than the zeta-potential in deionized water, but higher than OHA alone. Obviously, both lead ions and OHA are adsorbed on the perovskite surface. In addition, lead species that are adsorbed on the mineral surface act as reaction sites and can be chelated by OHA [30,43]. Meanwhile, the remaining lead in the solution will react with OHA to form a Pb-OHA complex that can be adsorbed on the surface of the perovskite and increase its hydrophobicity [30,44]. This is in accordance with the results of microflotation experiments.

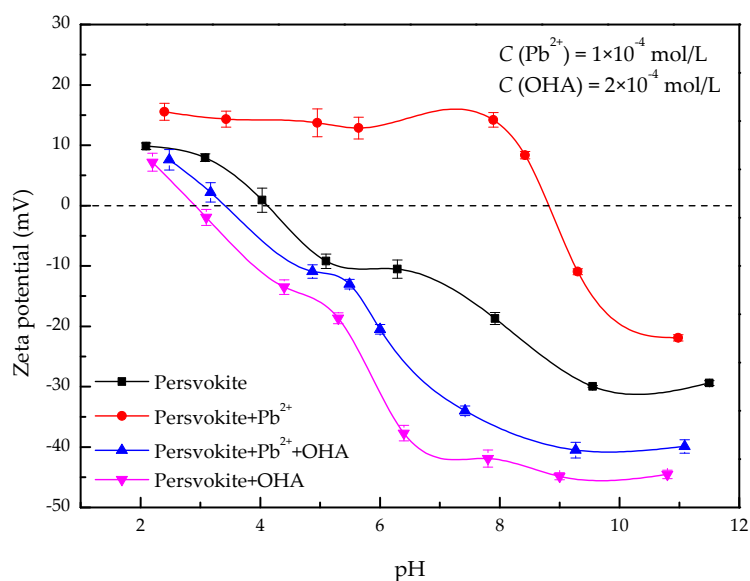


Figure 5. Zeta-potentials of perovskite as a function of pH.

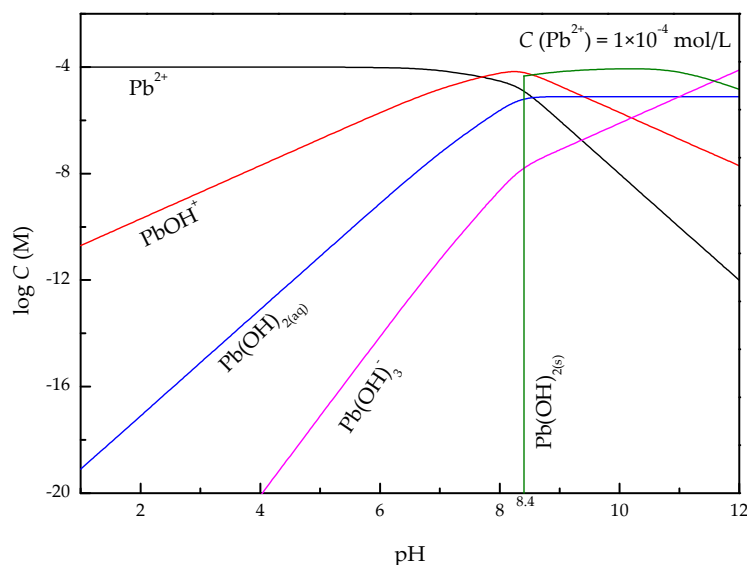


Figure 6. Logarithmic diagram of lead ions hydrolysis components.

3.3. Adsorption Tests

Figure 7 shows the effect of Pb^{2+} on adsorption of OHA on the perovskite surface. In the absence of Pb^{2+} , the effect of pH on OHA adsorption was not obvious; the adsorbance firstly increased, and then decreased with the increase of pH. In the presence of Pb^{2+} , the OHA adsorbance increased significantly with increasing pH, and the maximum adsorbance was reached at around pH 6.5. This can explain the results of the microflotation experiments. The results of the adsorption tests show that after activation with lead ions, the OHA adsorbance on the perovskite surface significantly increases in the investigated pH range, which indicates that the lead ions promote the adsorption of OHA on the perovskite surface. This may be attributed to an increase in the number of active sites and the formation of more stable Pb-OHA species on the perovskite surface [43,44].

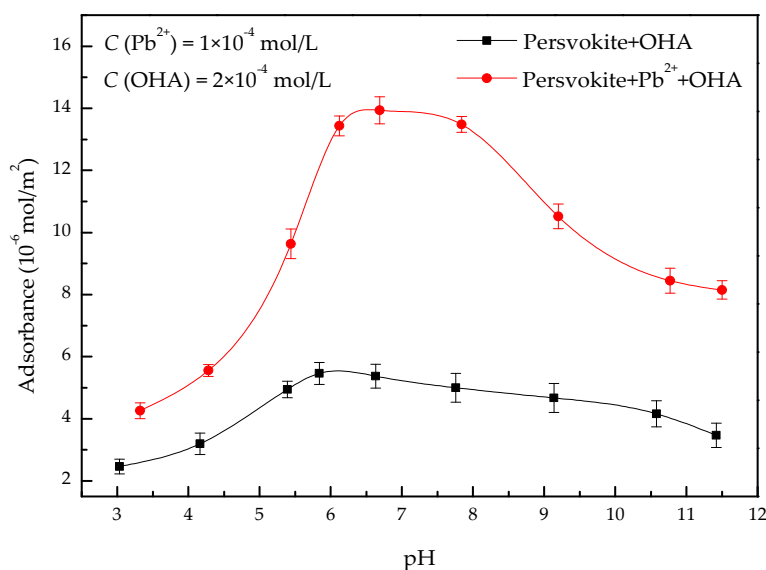


Figure 7. OHA adsorbance on the surface of perovskite as a function of pH.

3.4. FT-IR Analysis

Figure 8 shows the FT-IR spectra of perovskite before and after adjustment with different agents. In the infrared spectrum of OHA, the peak at 3248 cm^{-1} was due to the overlap of N–H and –OH stretching vibrations. The peaks at 3060 and 1561 cm^{-1} were attributed to the stretching vibration of N–H. Besides this, the peaks at 2944 , 2915 , 2846 , 1467 , 1423 , and 722 cm^{-1} were related to the stretching or bending vibrations of –CH₃ and –CH₂. Moreover, the peaks at 2763 , 1659 , 1620 , and 1116 cm^{-1} were derived from the stretching vibrations of –OH, C=O, C=N, and C=O. In addition, the absorption bands near 2400 cm^{-1} were characteristic of molecules containing long alkyl chains, because these bands came from the symmetrical and asymmetric stretching vibrations of the –CH₂– group. The absorption bands at 1077 , 1030 , and 969 cm^{-1} correspond to N–O stretching vibrations.

The infrared spectrum of perovskite shows two major bands at 565 and 448 cm^{-1} which belong to the characteristic peaks of Ti–O stretching and Ti–O–Ti bridge stretching modes. After treatment with OHA, the new peaks at 2919 cm^{-1} and 2851 cm^{-1} were related to the stretching vibration of C–H, and the band at 1448.9 cm^{-1} was the C–H antisymmetric deformation vibration of the –CH₃ group. The peak at 1116 cm^{-1} was the C=O stretching vibration. There was no significant change in these bands, but it was shown that OHA is adsorbed on the perovskite surface. The band at 1630 cm^{-1} was the stretching vibration of C=O, and that at 875 cm^{-1} was the stretching vibration of N–O. In addition, the shift of these peaks proves that OHA is adsorbed on the surface of the perovskite by chemical adsorption.

Infrared spectroscopy of the perovskite after treatment with lead ions and OHA shows that the stretching vibration peak of OH at 3433 cm^{-1} was significantly reduced, which contributed to the possible formation of metal coordination bonds. Furthermore, a new peak appeared at 2983 cm^{-1} , which corresponded to the asymmetric stretching vibration of –CH₃. In addition, the peak shifts at 1619 cm^{-1} and 1429 cm^{-1} were more significant, and the peaks at 2924 , 2854 , 1619 , 1429 , and 1124 cm^{-1} were more intense. Therefore, it can be speculated that the addition of Pb²⁺ enhances the adsorption of OHA on the perovskite surface.

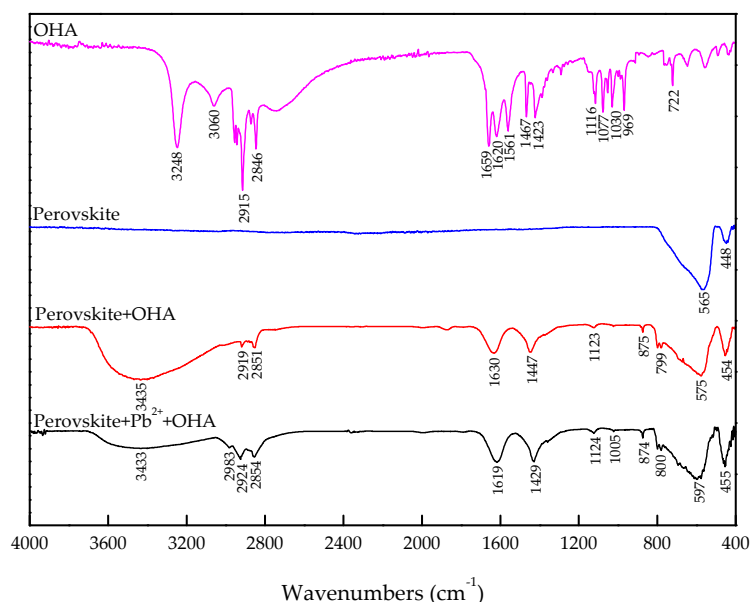


Figure 8. FT-IR spectra of perovskites before and after adjustment with different agents.

3.5. XPS Analysis

To further determine the interaction mechanism between OHA and perovskite activated with Pb²⁺, an XPS analysis of perovskite conditioned with Pb²⁺ ions or/and OHA was conducted. The relative

contents of the elements on the perovskite surface are summarized in Table 2. Table 2 shows that the Ti2p relative contents of the perovskite surface increased from 11.02% under a neutral condition, and to 13.48% under a weak acidic condition. Therefore, weak acidic conditions can increase the relative content of titanium sites on the perovskite surface. In addition, the Pb4f relative contents of the Pb²⁺-activated perovskite surface reached 0.44%, indicating that Pb²⁺ was successfully adsorbed on the perovskite surface. Furthermore, when OHA was added alone, the C1s and N1s relative contents were 49.37% and 0.55%. However, when perovskite was treated with Pb²⁺ and OHA, the relative contents of C1s and N1s increased by 9.07% and 0.31%, respectively. Thus, the adsorption of OHA is promoted by Pb²⁺.

Tables (Tables 3 and 4) present the binding energies and chemical shifts of elements on perovskite surfaces, respectively. After Pb²⁺ activation, the binding energies of Ti2p, Ca2p and O1s were shifted by −0.73, +0.07 and +0.35 eV, evidencing that the presence of Pb²⁺ changed the chemical circumstances of Ti and O species on the perovskite surface. When perovskite was treated with Pb²⁺ and OHA, the chemical shift of Ti2p was more significant, and significant chemical shifts were observed for Pb4f (−0.43 eV) and N1s (+0.71 eV) of perovskite treated with both Pb²⁺ and OHA, compared to that conditioned with Pb²⁺ or OHA alone. These confirm that more significant chemical reactions occur, and that the OHA could interact with lead species adsorbed on the surface of perovskite. This corresponds with the binding energy of Ca2p, which showed no obvious change after Pb²⁺ and OHA treatment.

The high-resolution XPS spectra of perovskite before and after Pb²⁺ and OHA treatment are shown in Figure 9. Figure 9a shows that the Ti2p3/2 peaks of pure perovskite appeared at around 458 eV, corresponding to the Ti⁴⁺ oxidation state [43]. After Pb²⁺ activation, the Ti2p3/2 binding energy decreased by 0.73 eV. The presence of Pb²⁺ ions changed the chemical circumstance of Ti species on the perovskite surface. Besides this, the addition of OHA further decreased the Ti2p3/2 binding energy to 457.71 eV, suggesting that OHA might bond with the Ti species of perovskite surfaces. Comparing with the N1s spectra without adding Pb²⁺ (Figure 9b), the N1s spectra treated by Pb²⁺ presented new peaks at 401.65 eV, which could be attributed to chemisorbed hydroxamates interacting with lead. The O1s XPS spectra recorded from pure perovskite, perovskite treated with Pb²⁺, and perovskite treated with both Pb²⁺ and OHA are shown in Figure 9c. The O1s peaks are composed of three components. The peaks at around 530.0 eV are attributed to Ti-O/Ti-O-Pb bonds [45,46], that at 531.5 eV attributed to Ca-O bonds [43,47], and that at 532.1 eV for hydroxyl bonded to metal ions (Me-OH) [46], respectively. The relative intensity of O1s peaks belonging to Ti-O bonds increased from 59.16% of pure perovskite to 59.60% of perovskite modified by Pb²⁺ and 63.55% of Pb²⁺-activated perovskite treated with OHA, while that of O-H bonds decreased from 14.23% to 11.41% and further to 7.40%. These results illustrated that lead species would interact with active Ti sites to form lead-containing complexes (Ti-O-Pb) on the perovskite surface. Consequently, lead species adsorbed on perovskite surfaces rendered new active sites for OHA adsorption. OHA replaced OH[−] ions and bonded to the active metal sites in the form of metal-hydroxamate chelate complexes, improving the hydrophobicity of perovskite.

Table 2. Relative contents of elements on the perovskite surface.

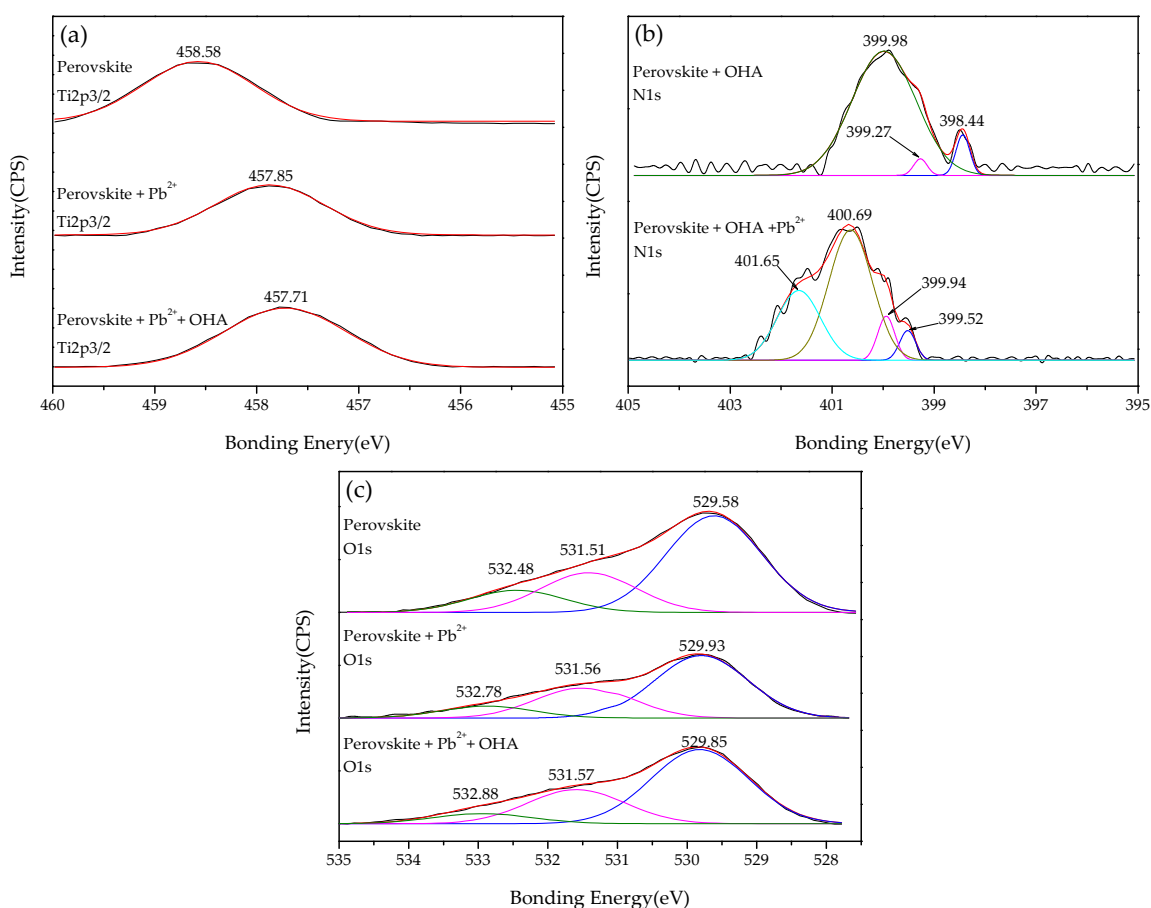
Sample	Surface Atomic Composition (%)					
	C1s	Ti2p	Ca2p	O1s	Pb4f	N1s
Perovskite	43.18	11.02	7.72	36.69	-	-
Perovskite (pH = 6.5)	33.37	13.48	8.49	43.10	-	-
Perovskite + Pb ²⁺ (pH = 6.5)	37.64	12.58	8.35	39.86	0.44	
Perovskite + OHA (pH = 6.5)	49.37	10.05	6.43	32.02		0.55
Perovskite + Pb ²⁺ + OHA (pH = 6.5)	58.44	8.08	5.33	26.24	0.52	0.86

Table 3. Binding energies of elements on the perovskite surface.

Sample	Binding Energy (eV)					
	C1s	Ti2p	C1s	O1s	C1s	N1s
Perovskite	284.78	458.58	346.48	529.58	-	-
Perovskite + Pb ²⁺	284.77	457.85	346.55	529.93	138.50	-
Perovskite + OHA	284.73	458.07	346.57	529.83	-	399.98
Perovskite + Pb ²⁺ + OHA	284.75	457.71	346.54	529.85	138.16	400.69

Table 4. Chemical shifts of the elemental binding energies of the perovskite surface.

Sample	Chemical Shift (eV)					
	C1s	Ti2p	Ca2p	O1s	Pb4f	N1s
Perovskite + Pb ²⁺	-0.01	-0.73	+0.07	+0.35	-	-
Perovskite + OHA	-0.05	-0.51	+0.09	+0.25	-	-
Perovskite + Pb ²⁺ + OHA	-0.03	-0.87	+0.06	+0.27	-0.34	+0.71

**Figure 9.** High-resolution XPS spectra of perovskite before and after Pb²⁺ and OHA treatment: (a) Ti2p, (b) N1s, (c) O1s. (Black line: original curve, red line: fitted curve, other colors line: curve of XPS-peak-differentiation-imitating analysis)

4. Discussion

According to the experimental results and analyses, the presence of Pb²⁺ can promote the adsorption of OHA and enhance the flotability of perovskite. The results of microflotation and adsorption tests indicate that the presence of Pb²⁺ can promote the adsorption of OHA on the perovskite

surface and enhance the flotability of perovskite in a wide pH range. The zeta-potential analysis shows that specific adsorption of OHA and lead species on the perovskite surface can occur. The adsorption of Pb^{2+} and $PbOH^+$ on the perovskite surface makes the zeta-potential of perovskite shift positively in the pH range from 6.0 to 7.0, which is in agreement with the results of microflotation and adsorption tests. The FT-IR results give further evidence that OHA can chemisorb onto the surface of perovskite, and that the addition of Pb^{2+} can enhance the adsorption of OHA on the perovskite surface. The XPS analysis shows that the addition of Pb^{2+} can change the chemical circumstances of Ti and O species on the perovskite surface. When perovskite is treated with both Pb^{2+} and OHA, the binding energies of Ti2p, Pb4f, O1s and N1s present significant shifts (0.27–0.87 eV). Thus, it can be inferred that the Pb^{2+} and $PbOH^+$ are adsorbed onto the surface of perovskite, which increases the number of activated sites. Then, the OHA molecules and anions would chelate with Ti or Pb on the perovskite surface; besides this, the nonpolar part of the OHA species adsorbs the former OHA species by a hydrogen bond, which is consistent with the results of the zeta-potentials and FT-IR.

Based on these results, it can be concluded that Pb^{2+} can promote perovskite flotation effectively by using OHA as collector. It can be considered that the lead species are adsorbed on the perovskite surface first, and then the Ti and Pb reacted with OHA to form hydrophobic species of metal-OHA complexes; besides this, the nonpolar part of the OHA species adsorb the former OHA species by a hydrogen bond. This promotes the adsorption of OHA on the perovskite surface and enhances the flotability of perovskite. The adsorption model of Pb^{2+} and OHA on the perovskite surface in Figure 10 reveals the potential mechanism of Pb^{2+} activation and OHA adsorption.

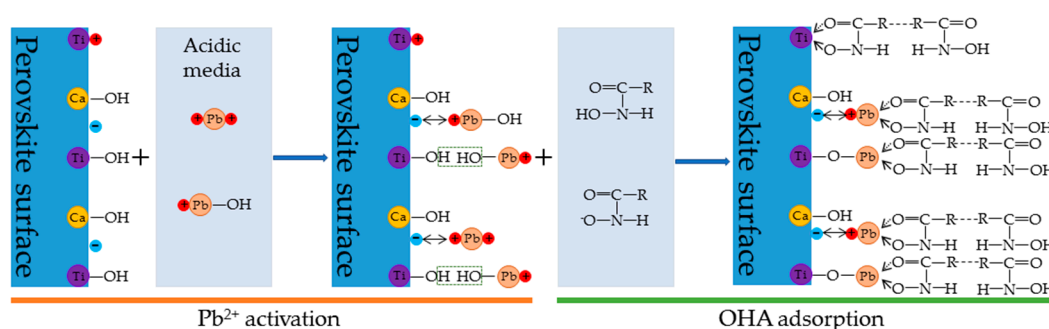


Figure 10. Proposed adsorption model of Pb^{2+} and OHA on the perovskite surface.

5. Conclusions

1. In the present study, the effects of lead ions on the perovskite flotability and the activation mechanism of lead ions in perovskite flotation with an octyl hydroxamic acid collector were investigated using microflotation experiments, zeta-potential measurements, adsorption tests, FT-IR, and XPS analyses. The results of microflotation and adsorption tests indicate that the presence of Pb^{2+} can promote the adsorption of OHA on the perovskite surface and enhance the flotability of perovskite in a wide pH range. In addition, maximum recovery of 79.62% could be obtained at pH 6.5 in the presence of Pb^{2+} .
2. The zeta-potential shows that specific adsorption of OHA and lead species on the perovskite surface can occur. FT-IR and XPS measurements indicate that the adsorption of lead ions on the perovskite surface is mainly chemical adsorption. FT-IR analysis gives further evidence that the lead species react with titanium hydroxyl compounds on the perovskite surface to form lead complexes, which are the main active sites for OHA adsorption. Meanwhile, FT-IR and XPS analyses confirm that OHA chemisorbs on the surface of Pb^{2+} -activated perovskite and forms hydrophobic Pb-OHA complexes, and then the nonpolar part of OHA species molecules will adsorb the nonpolar part of the former OHA species through hydrogen bonds to form multi-layer adsorption. This adsorption mode improves the flotability of perovskite.

Author Contributions: W.W. and Y.Z. conceived and designed the experiments; Y.Z. performed the experiments; Y.Z. and Y.C. analyzed the data; W.W. contributed reagents and materials; Y.Z. wrote the paper.

Funding: This research was funded by [Fund of the State Key Laboratory of Mineral Processing] grant number [BGRIMM-KJSKL-2015-07], [the Opening Project of Key Laboratory of Solid Waste Treatment and Resource Recycling, Ministry of Education] grant number [13zxsk06], [Postgraduate Innovation Fund Project of the Southwest University of Science and Technology] grant number [18ycx044]. And the APC was funded by [Southwest University of Science and Technology].

Acknowledgments: This study was financially supported by the Fund of the State Key Laboratory of Mineral Processing (BGRIMM-KJSKL-2015-07), the Opening Project of Key Laboratory of Solid Waste Treatment and Resource Recycling, Ministry of Education (13zxsk06), and the Postgraduate Innovation Fund Project of the Southwest University of Science and Technology (18ycx044).

Conflicts of Interest: The authors declare no conflict of interest.

References

1. Bulatovic, S.; Wyslouzil, D.M. Process development for treatment of complex perovskite, ilmenite and rutile ores. *Miner. Eng.* **1999**, *12*, 1407–1417. [[CrossRef](#)]
2. Chen, D.S.; Zhao, L.S.; Qi, T.; Hu, G.P.; Zhao, H.X.; Li, J.; Wang, L.N. Desilication from titanium–vanadium slag by alkaline leaching. *Trans. Nonferr. Met. Soc.* **2013**, *23*, 3076–3082. [[CrossRef](#)]
3. Samal, S.; Mohapatra, B.K.; Mukherjee, P.S.; Chatterjee, S.K. Integrated XRD, EPMA and XRF study of ilmenite and titania slag used in pigment production. *J. Alloys Compd.* **2009**, *474*, 484–489. [[CrossRef](#)]
4. Zhang, J.L.; Xing, X.D.; Cao, M.M.; Jiao, K.X.; Wang, C.L.; Ren, S. Reduction kinetics of vanadium titano-magnetite carbon composite pellets adding catalysts under high temperature. *J. Iron Steel Res. Int.* **2013**, *20*, 1–7. [[CrossRef](#)]
5. Hou, T.; Zhang, Z.; Ye, X.; Encarnacion, J.; Reichow, M.K. Noble gas isotopic systematics of Fe–Ti–V oxide ore-related mafic–ultramafic layered intrusions in the Panxi area, China: The role of recycled oceanic crust in their petrogenesis. *Geochim. Cosmochim. Acta* **2011**, *75*, 6727–6741. [[CrossRef](#)]
6. Kothari, N.C. Recent developments in processing ilmenite for titanium. *Int. J. Miner. Process.* **1974**, *1*, 287–305. [[CrossRef](#)]
7. Noguchi, H.; Natsui, S.; Kikuchi, T.; Suzuki, R.O. Reduction of CaTiO₃ by electrolysis in the molten salt CaCl₂–CaO. *Electrochemistry* **2018**, *86*, 82–87. [[CrossRef](#)]
8. Pan, F.; Zhu, Q.S.; Zhan, D.U.; Sun, H.Y. Oxidation kinetics, structural changes and element migration during oxidation process of vanadium–titanium magnetite ore. *J. Iron Steel Res. Int.* **2016**, *23*, 1160–1167. [[CrossRef](#)]
9. Han, G.H.; Tao, J.; Zhang, Y.B.; Huang, Y.F.; Guang-Hui, L.I. High-temperature oxidation behavior of vanadium, titanium-bearing magnetite pellet. *J. Iron Steel Res. Int.* **2011**, *18*, 14–19. [[CrossRef](#)]
10. He, S.; Sun, H.; Tan, D.G.; Peng, T. Recovery of titanium compounds from Ti-enriched product of alkali melting Ti-bearing blast furnace slag by dilute sulfuric acid leaching. *Procedia Environ. Sci.* **2016**, *31*, 977–984. [[CrossRef](#)]
11. Zhang, L.; Zhang, L.N.; Wang, M.Y.; Li, G.Q.; Sui, Z.T. Recovery of titanium compounds from molten Ti-bearing blast furnace slag under the dynamic oxidation condition. *Miner. Eng.* **2007**, *20*, 684–693. [[CrossRef](#)]
12. Niu, Y.; Du, X.; Yang, W.; Sui, Z. Flotation of the modified high titanium bf slag. *J. Mater. Met.* **2012**, *11*, 13–17. (In Chinese)
13. Li, J.; Zhang, Z.T.; Wang, X.D. Precipitation behaviour of Ti enriched phase in Ti bearing slag. *Ironmak. Steelmak.* **2000**, *39*, 414–418. [[CrossRef](#)]
14. Jiang, K.; Hu, X.; Ma, M.; Wang, D.; Qiu, G.; Jin, X.; Chen, G.Z. “Perovskitization”-assisted electrochemical reduction of solid TiO₂ in molten CaCl₂. *Angew. Chem. Int. Ed.* **2006**, *45*, 428–432. [[CrossRef](#)] [[PubMed](#)]
15. Lou, T.; Li, Y.H.; Li, L.S.; Sui, Z. Study of precipitation of perovskite phase from the oxide slag. *Acta Metall. Sin.* **2000**, *36*, 141–144. (In Chinese)
16. Li, L.; Sui, Z. Physical chemistry behavior of enrichment selectivity of TiO₂ in perovskite. *Acta Phys.-Chim. Sin.* **2001**, *17*, 845–849. (In Chinese)
17. Wang, W.; Zhu, Y.; Zhang, S.; Deng, J.; Huang, Y.; Yan, W. Flotation behaviors of perovskite, titanite, and magnesium aluminate spinel using octyl hydroxamic acid as the collector. *Minerals* **2017**, *7*, 134. [[CrossRef](#)]

18. Zhang, S. Study on High-Temperature Enrichment and Flotation Separation of Titanium Components from Ti-Bearing Blast Furnace Slag. Master's Thesis, Southwest University of Science and Technology, Mianyang, Sichuan, China, 2017; pp. 43–47. (In Chinese)
19. Meng, Q.; Feng, Q.; Shi, Q.; Ou, L. Studies on interaction mechanism of fine wolframite with octyl hydroxamic acid. *Miner. Eng.* **2015**, *79*, 133–138. [[CrossRef](#)]
20. Wu, X.Q.; Zhu, J.G. Selective flotation of cassiterite with benzohydroxamic acid. *Miner. Eng.* **2006**, *19*, 1410–1417. [[CrossRef](#)]
21. Liu, B.; Wang, X.; Du, H.; Liu, J.; Zheng, S.; Zhang, Y.; Miller, J.D. The surface features of lead activation in amyl xanthate flotation of quartz. *Int. J. Miner. Process.* **2016**, *151*, 33–39. [[CrossRef](#)]
22. Crumbliss, A.L. Iron bioavailability and the coordination chemistry of hydroxamic acids. *Coord. Chem. Rev.* **1990**, *105*, 155–179. [[CrossRef](#)]
23. Chen, G.L.; Tao, D.; Ren, H.; Ji, F.F.; Qiao, J.K. An investigation of niobite flotation with octyl diphosphonic acid as collector. *Int. J. Miner. Process.* **2005**, *76*, 111–122. [[CrossRef](#)]
24. Agrawal, Y.K. Hydroxamic acids and their metal complexes. *Russ. Chem. Rev.* **1979**, *48*, 948–963. [[CrossRef](#)]
25. Ni, X.; Liu, Q. The adsorption and configuration of octyl hydroxamic acid on pyrochlore and calcite. *Colloids Surf. A* **2012**, *411*, 80–86. [[CrossRef](#)]
26. Abaka-Wood, G.B.; Addai-Mensah, J.; Skinner, W. A study of selective flotation recovery of rare earth oxides from hematite and quartz using hydroxamic acid as a collector. *Adv. Powder Technol.* **2018**, *29*, 1886–1899. [[CrossRef](#)]
27. Pavez, O.; Brandao, P.R.G.; Peres, A.E.C. Adsorption of oleate and octyl-hydroxamate on to rare-earth minerals. *Miner. Eng.* **1996**, *9*, 357–366. [[CrossRef](#)]
28. Zhang, W.; Honaker, R.Q.; Groppo, J.G. Flotation of monazite in the presence of calcite part I: Calcium ion effects on the adsorption of hydroxamic acid. *Miner. Eng.* **2017**, *100*, 40–48. [[CrossRef](#)]
29. Zhang, W.; Honaker, R.Q. Flotation of monazite in the presence of calcite part II: Enhanced separation performance using sodium silicate and EDTA. *Miner. Eng.* **2018**. [[CrossRef](#)]
30. Xu, L.; Tian, J.; Wu, H.; Lu, Z.; Yang, Y.; Sun, W.; Hu, Y. Effect of Pb^{2+} ions on ilmenite flotation and adsorption of benzohydroxamic acid as a collector. *Appl. Surf. Sci.* **2017**, *425*, 796–802. [[CrossRef](#)]
31. Fan, X.; Rowson, N.A. The effect of $Pb(NO_3)_2$ on ilmenite flotation. *Miner. Eng.* **2000**, *13*, 205–215. [[CrossRef](#)]
32. Li, H.; Mu, S.; Weng, X.; Zhao, Y.; Song, S. Rutile flotation with Pb^{2+} ions as activator: Adsorption of Pb^{2+} at rutile/water interface. *Colloids Surf. A* **2016**, *506*, 431–437. [[CrossRef](#)]
33. Han, H.; Hu, Y.; Sun, W.; Li, X.; Cao, C.; Liu, R.; Yue, T.; Meng, X.; Guo, Y.; Wang, J. Fatty acid flotation versus BHA flotation of tungsten minerals and their performance in flotation practice. *Int. J. Miner. Process.* **2017**, *159*, 22–29. [[CrossRef](#)]
34. Liu, C.; Feng, Q.; Zhang, G.; Ma, W.; Meng, Q.; Chen, Y. Effects of lead ions on the flotation of hemimorphite using sodium oleate. *Miner. Eng.* **2016**, *89*, 163–167. [[CrossRef](#)]
35. Yang, S.; Qiu, X.; Peng, T.; Chang, Z.; Feng, Q.; Zhong, C. Beneficial effects and mechanism of lead ion on wolframite flotation. *Physicochem. Probl. Miner. Process.* **2016**, *52*, 855–873.
36. Kay, H.F.; Bailey, P.C. Structure and properties of $CaTiO_3$. *Acta Crystallogr.* **1957**, *10*, 219–226. [[CrossRef](#)]
37. Mehdilo, A.; Irannajad, M.; Rezai, B. Effect of crystal chemistry and surface properties on ilmenite flotation behavior. *Int. J. Miner. Process.* **2015**, *137*, 71–81. [[CrossRef](#)]
38. Fan, X.; Waters, K.E.; Rowson, N.A.; Parker, D.J. Modification of ilmenite surface chemistry for enhancing surfactants adsorption and bubble attachment. *J. Colloid Interface Sci.* **2009**, *329*, 167–172. [[CrossRef](#)] [[PubMed](#)]
39. Kurzak, B.; Kozłowski, H.; Farkas, E.; Kurzak, B.; Kozłowski, H.; Farkas, E. Hydroxamic and aminohydroxamic acids and their complexes with metal ions. *Coord. Chem. Rev.* **1992**, *114*, 169–200. [[CrossRef](#)]
40. Sreenivas, T.; Padmanabhan, N.P.H. Surface chemistry and flotation of cassiterite with alkyl hydroxamates. *Colloids Surf. A Physicochem. Eng. Asp.* **2002**, *205*, 47–59. [[CrossRef](#)]
41. Marabini, A.M.; Ciriachi, M.; Plescia, P.; Barbaro, M. Chelating reagents for flotation. *Miner. Eng.* **2007**, *20*, 1014–1025. [[CrossRef](#)]
42. Zhang, W.; Honaker, R. A fundamental study of octanohydroxamic acid adsorption on monazite surfaces. *Int. J. Miner. Process.* **2017**, *164*, 26–36. [[CrossRef](#)]
43. Meng, Q.; Yuan, Z.; Yu, L.; Xu, Y.; Du, Y. Study on the activation mechanism of lead ions in the flotation of ilmenite using benzyl hydroxamic acid as collector. *J. Ind. Eng. Chem.* **2018**, *62*, 209–216. [[CrossRef](#)]

44. Han, H.S.; Liu, W.L.; Hu, Y.H.; Sun, W.; Li, X.D. A novel flotation scheme: Selective flotation of tungsten minerals from calcium minerals using Pb–BHA complexes in Shizhuyuan. *Rare Met.* **2017**, *36*, 533–540. [[CrossRef](#)]
45. Ouerd, A.; Alemany-Dumont, C.; Berthomé, G.; Normand, B.; Szunerits, S. Reactivity of titanium in physiological medium I. Electrochemical characterization of the metal/protein interface. *J. Electrochem. Soc.* **2007**, *35*, C593–C601. [[CrossRef](#)]
46. Soccol, D.; Martens, J.; Claessens, S.; Fransaer, J. Effect of carbon modification of particles on their incorporation rate during electrodeposition. *J. Electrochem. Soc.* **2011**, *158*, D515–D523. [[CrossRef](#)]
47. Feng, Q.; Zhao, W.; Wen, S.; Cao, Q. Activation mechanism of lead ions in cassiterite flotation with salicylhydroxamic acid as collector. *Sep. Purif. Technol.* **2017**, *178*, 193–199. [[CrossRef](#)]



© 2018 by the authors. Licensee MDPI, Basel, Switzerland. This article is an open access article distributed under the terms and conditions of the Creative Commons Attribution (CC BY) license (<http://creativecommons.org/licenses/by/4.0/>).